



Experimental Study on Transient Characteristics of Grounding Grid for Substation

DUAN Lian, ZHANG Bo, HE, Jinliang

Department of Electrical Engineering, Tsinghua University
Beijing, 10084, China
line 4: duanl15@mails.tsinghua.edu.cn

XIAO Leishi, LI Qian

Electric Power Research Institute, Guangdong Power Grid
Company
Guangzhou, 510080, China

Abstract—Previous work has proven that transient characteristics of a grounding grid was far more different than its performance at power frequency because of the inductance of the system and the soil ionization phenomena. In this paper, a test on a grounding grid of a 110 kV substation was conducted. Several parameters, such as waveform, peak value and injecting point of lightning, were altered to study their relationship with transient characteristics. Not only the impulse earthing resistance but also the voltage and current distribution of the conductors were analyzed. Characteristics of grounding grid between power frequency and higher frequency were compared.

Keywords—field test; substation grounding system; impulse transient characteristic; lightning impulse

I. INTRODUCTION

The safe and reliable operation of a substation has a close relationship with the performance of grounding system. When the substation is struck by a lightning, the characteristics of the grounding system subject to the high impulse current is dramatically different from that at the low frequency [1]-[2]. As the frequency rises, the inductive component in the system would play a more important role. Under this condition, current would dissipate into the soil concentrated close to the feeding point, thus causing an uneven potential distribution that would threaten the electronic equipment and power apparatus in the station. In order to design a suitable earthing system, it is fundamental to study its impulse performance.

In recent years, based on the circuit method, transmission line method [3]-[8], and electromagnetic-field approaches[9]-[18], computer simulation technologies are now relatively mature that could take soil ionization and mutual inductive impedance into account. However, physical phenomenon in real lightning case is such a complicated process that no model is able to thoroughly explain the complete situation [19]. Therefore, the field test is necessary because it could more comprehensively imitate the real-case situation. Yet, for the reason that impulse current generator is too big to move to the field test location and the experimental condition is too complex, the testing current of most impulse test is very small [10], and their tested earthing device is so small that could not simulate all the phenomenon [20] [22].

In this paper, impulse current up to several kilo amperes is fed into a grounding system of a 110 kV substation with an

area of 50 m × 52.5 m. The impulse characteristic, including not only the transient grounding resistance and its impulse GPR waveform but also the voltage distribution of the whole grounding system, is measured. The effect of several parameters, such as current feeding position, amplitude of the current and front time of the waveform on the transient performance are studied. Research in this paper comprehensively reveals the transient characteristic of a 110 kV substation grounding system and could be used as basic data, which will be helpful to check numerical simulation results.

II. BASIC LAYOUT OF THE TEST

A. Grounding Size and Soil Parameters

Figure 1. illustrates the grounding system for the experiment, which belongs to a full size 110 kV substation. This grounding system includes a main mesh sized by 50 m × 52.5 m that could be divided into 4 sub-grids and an earthing system sized by 14 m × 45.5 m used for controlling room (solid lines) where the impulse current generator is set up. The grounding system is buried 0.8 m deep and made of steel with radius of 22 mm.

Soil resistivity was measured by Wenner method using SYSCAL soil analyzer. Distance of the pole and corresponding apparent resistance were recorded in TABLE II. After calculation, soil in this experiment field could be characterized by a 3-layer horizontal model. Corresponding parameters were shown in TABLE II.

TABLE I. SOIL MEASUREMENT

Pole Distance(m)	Apparent Resistance (Ω)	Apparent Soil Resistivity (Ω·m)
20	2.130	267.528
15	3.240	305.208
13	3.940	321.662
10	5.500	345.400
8	7.030	353.187
6	8.970	337.990
4	12.540	315.005
3	15.310	288.440
2	17.430	218.921
1	20.090	126.165
0.5	31.710	99.569

TABLE II. SOIL PARAMETERS

Layer No.	Thickness (m)	Soil Resistivity ($\Omega \cdot m$)
1	0.844	88.13
2	2.89	807.62
3	infinite	213.01

B. Testing Layout

The generator is propped up by several pillars to make sure it is insulated from the ground. For contrasting reason, border and center of the main grid both are chosen as the injecting points. Position are shown in Figure 1. indicated as blue circles, named as A1 and B1 respectively. The current-return pole is composed of two 37 m grounding electrodes crossing together 52.5 m away from bottom the grid, as shown in Figure 1. In order to reduce the inductive coupling between the current lead and the potential lead, the voltage reference point was set to the left of the grounding grid with a distance of 160 m.

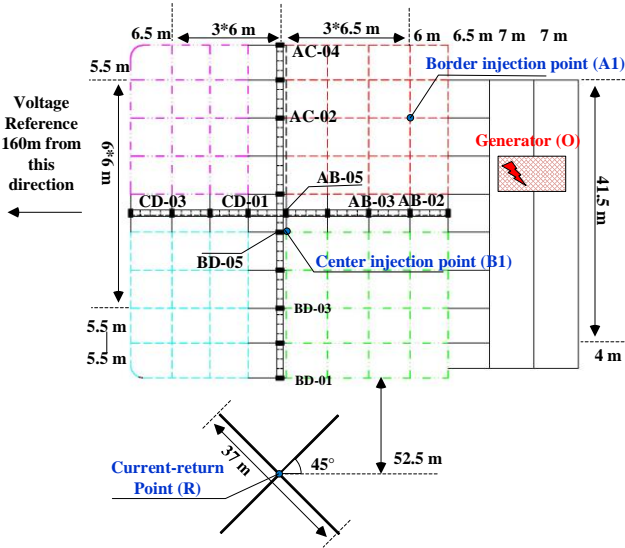


Figure 1. Simplified layout of the testing field

According to computer simulation, when feeding a 1 kA 8/20 μs impulse current from point B1, the arrangement of the current-return pole and voltage reference point would cause the impulse resistance to decrease from 2.4 to 2.2 Ω . The error was 8.33%, which seems acceptable for field test.

C. Equipment Parameters and Observation Points

The impulse current generator has three charging stages and each of them had 300 kV maximum charging voltage. The overall charging voltage is 900 kV and is capable to generate impulse current up to 30 kA under a load of 4 Ω . Only the charging voltage could be set directly that controlled the current amplitude. In this test, two types of waveform, 8/20 μs and 2.6/50 μs , are chosen and under each waveform the limit of single-stage charging voltage is set to 100 kV. In this circumstance, maximum peak current of 8/20 μs is about 5 kA while that of 2.6/50 μs is 1 kA.

Voltage dividers and Pearson current sensors are used to measure voltages and currents. Several Yokogawa 850/750 16-channel oscilloscopes are used to store the waveform. Since each channel is independent and power by UPS, interference could be limit to the minimum level.

The emphasis of this paper is not only on the impulse GRP waveform and transient resistance but also on the potential and current distribution on the grounding conductors under transient condition. Therefore, more than one measuring point should be set.

The voltage measured from the current injecting points is the impulse GPR of the whole earthing system, with which transient resistance could be easily calculated. Those boxes on the center cross of the grounding grids with name tags next to it are used as observation points to reflect the potential distribution of the testing grounding system.

III. IMPULSE CHARACTERISTIC OF THE GROUNDING MESH

The characteristic of grounding grid discussed in this paper includes transient GPR and resistance together with impulse voltage distribution. According to the testing circuit layout described in section II, with current-return pole and voltage reference point fixed, altering feeding position, peak value of the current and different waveform could brought multiple sets of data expressing the impulse characteristic of the grounding mesh.

A. Impulse GPR Waveform and Transient Resistance

1) Influence of the feeding position

Two sets of data are shown in Figure 2. when the same 8/20 μs current is sent into the grid at different position. There is an obvious difference between the maximum values of the two GPRs but the rise time of the two GPRs are about the same and they are ahead of current.

When injecting from the center, the current peak value is 3.65 kA at 10.5 μs , creating a GPR with a peak of 7.33 kV at 5.1 μs . In contrast, when injection point changes to the border, the peak value of the current is 3.883 kA at 10.1 μs and the GPR is 9.74 kV at 5 μs . Although when injected from the corner, the current has only increased 6.4%, the GPR rises 32.9%.

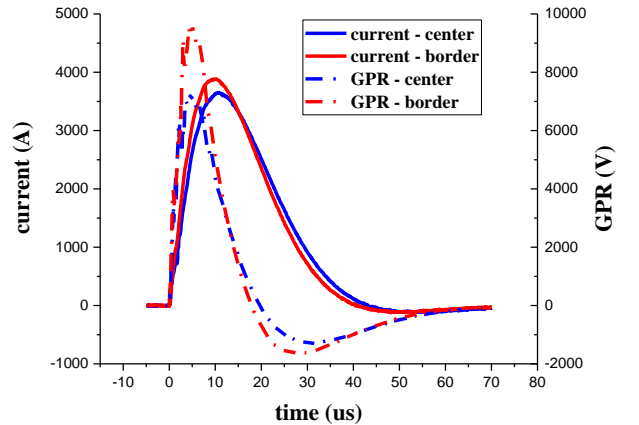


Figure 2. Injecting current and grid GRP with different injecting positions

Rise time of GPR is ahead of that of the feeding current is due to inductive effect. The leading time in this case was around $5 \mu\text{s}$ and irrelevant to injecting position. For simple definition, the transient resistance is the ratio of the amplitude of GPR and that of the current even they are not at the same time [2]. As the injecting position changes from center to border, the transient resistance increases from 2.01Ω to 2.51Ω . When lightning strikes on the center of the grid, it is more easily for the impulse current to flow into the earth along the conductors because all the directions can be used. This proves that when current's injecting from the center, grounding grid has a larger effective area [22].

2) Influence of the testing waveform

In this case, influence of the waveform is studied. In order to get different waveforms, resistor and inductor configuration on the generator has to be altered. Therefore, current amplitudes of different waveforms in this section could not be exactly the same. However, even the amplitude of $2.6/50 \mu\text{s}$ is lower than that of $8/20 \mu\text{s}$, its GPR peak value is considerably higher.

Two sets of data with similar injecting amplitudes are picked in Figure 3. Both of them are fed into the center of the center of the grounding grid. $8/20 \mu\text{s}$ has a peak value of 1.19 kA at $9.4 \mu\text{s}$ while $2.6/50 \mu\text{s}$ has a peak value of 0.74 kA at $3.2 \mu\text{s}$. Peak value of GPR caused by the 1.19 kA $8/20 \mu\text{s}$ current is 2.63 kV , appearing at $5.2 \mu\text{s}$. Corresponding to $8/20 \mu\text{s}$, GPR brought by $2.6/50 \mu\text{s}$ has a maximum value of 4.66 kV at $0.8 \mu\text{s}$. For $8/20 \mu\text{s}$ waveform, peak time of GPR is 44.68% ahead of that of the current; for $2.6/50 \mu\text{s}$ waveform, this percentage is 75% . Therefore, impulse grounding resistance calculated by $8/20 \mu\text{s}$ waveform is 2.21Ω . In contrast, when $2.6/50 \mu\text{s}$ testing waveform is used, it rises to 6.30Ω .

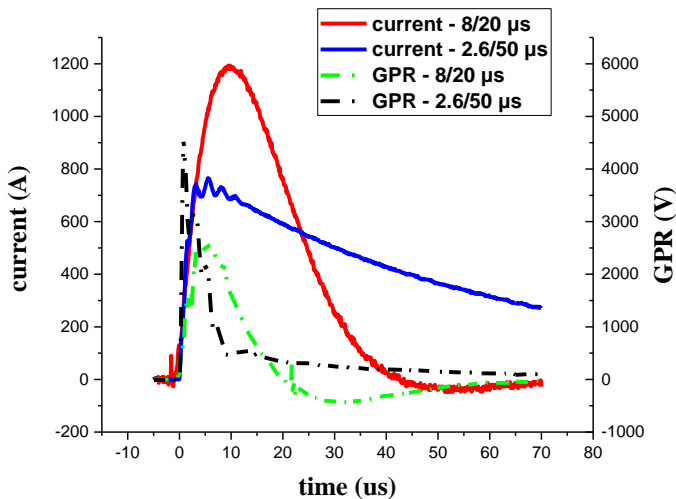


Figure 3. Injecting current and grid GRP with different waveforms

When the testing waveform becomes steeper, it contains more high frequency component, thus bringing a higher impedance to the earthing system, which is the reason why $2.6/50 \mu\text{s}$ current has a higher impulse resistance and a more leading GPR peak time.

3) Influence of the impulse current amplitude

In this section, three sets of tests are compared. During one of them, $8/20 \mu\text{s}$ currents with different amplitudes by changing the single-stage charging voltage from 30 kV to 100 kV are injected from the center. The other two sets are different from the injecting point and waveform respectively. In Figure 4, apparently all the three sets of data has the same trend that as impulse current increased, transient resistances decreased.

When $8/20 \mu\text{s}$ current injects in the center, the impulse resistance of 1.19 kA is 2.21Ω while that of 4.04 kA is 1.88Ω , having a decrease of 14.9% . For the second circumstance that $8/20 \mu\text{s}$ current is fed at the border, the resistance reduced from 3.01Ω to 2.52Ω , cut down by 16.3% . Since it is very difficult for the generator to output a $2.6/50 \mu\text{s}$ impulse current with a high amplitude, the maximum amplitude of the current in this test is 0.863 kA , even the single-stage charging voltage is 90 kV . The resistance debases from 7.82Ω to 5.97Ω by 23.66% .

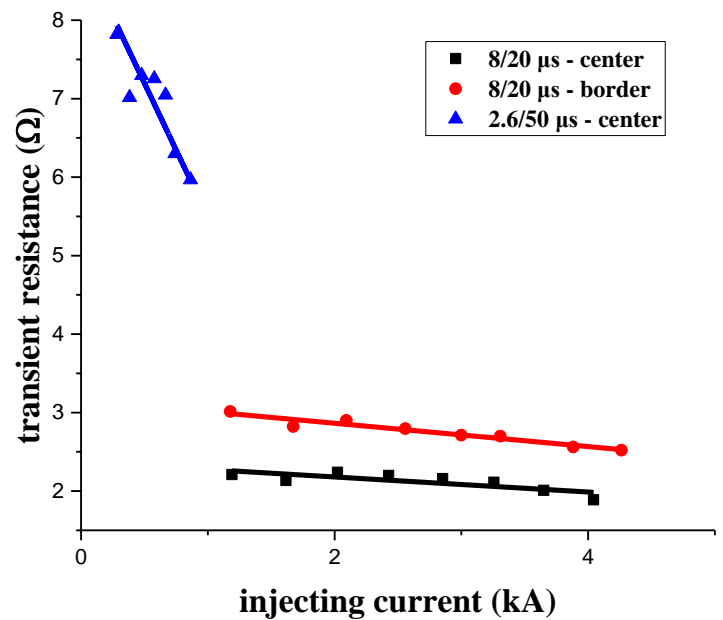


Figure 4. Transient resistance with different current amplitudes

The soil ionization is the reason of the decreasing trend of impulse resistance. When $2.6/50 \mu\text{s}$ waveform is used, the phenomenon is even more so although current amplitude was under 1 kA . Under $2.6/50 \mu\text{s}$ condition, the frequency is so high that the grounding reactance goes up tremendously, which makes the current disperse into the soil more concentrative to injecting position, further debasing the effective area of the grounding system. Even the feeding current does not have an absolutely high amplitude, soil is easy to be ionized.

B. Impulse voltage distribution on grounding grids

Unlike the power-frequency characteristic, the impulse voltage distribution on the grounding conductors varies a lot. According to the diagram in Figure 1, voltage amplitude of the

observation points on the crossing lines in the center are recorded. Considering symmetry, only vertical direction is included in this analysis. Horizontal coordinate is the distance to the injecting point. For those observation points above the injecting point, the distances are negative. Distances on the other side are positive.

1) Influence of the injecting position

Two sets of data with the same 8/20 μ s impulse current injecting from different places are picked. The current amplitudes of center and border injected were 4.043 kA and 4.263 kA respectively. The voltage amplitudes of horizontal observations is shown in Figure 5.

When lightning current is injecting from the center, the peak value voltage of the center is 7.9 kV, significantly higher than other 4 observations, the amplitudes of which are around 6 kV. However, when lightning current was injecting from the border of the grids, the GPR distribution is flatter. The points on the left side has a little bit higher amplitudes.

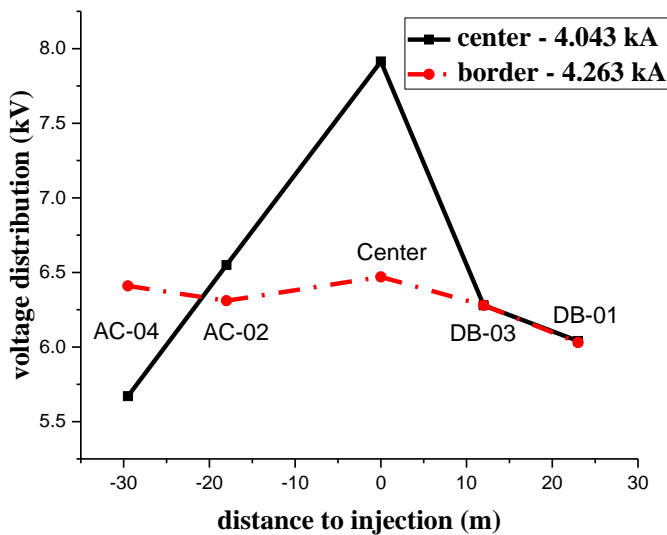


Figure 5. Voltage distribution of horizontal observations with different injecting position

It could be concluded that voltage of conductors near the injecting point has an uneven distribution. Because in the effective area of the grounding system, conductor potential has a great difference, according to the concept discussed in [22]. In this case, the imbalance level was 27.8%, which is defined as $(V_{max} - V_{min}) / V_{max}$.

2) Influence of the testing waveform

In this section, comparison of voltage distribution is made between the data during different waveforms. The current amplitudes of 8/20 μ s and 2.6/50 μ s are 1.153 and 0.977 kA respectively. The peak value of voltages of horizontal observations are shown in Figure 6.

The maximum values of the currents are almost the same, but the potential of the conductors are dramatically different. As the rise time of the waveform becomes shorter, the potential

near the injection position rises significantly and that far away from the center decreases a little, which makes the whole imbalance level even worse. In this situation, the imbalance level of 2.6/50 μ s is 73.0% while that of 8/20 μ s is 22.1%

3) Influence of the impulse current amplitude

Waveform and injecting position are kept fixed in this section and only the relation between voltage distribution and current amplitude is studied. Set the single-stage charging voltage to 30 kV, 40 kV, 60 kV, 80 kV and 100 kV respectively and the current corresponded are 1.153 kA, 1.617 kA, 2.427 kA, 3.257 kA and 4.043 kA.

As shown in Figure 7, when the amplitude of the currents injected increases, voltages of all the conductors rises simultaneously with the same ratio, which means that effective area of the grounding system does not change with the current amplitude.

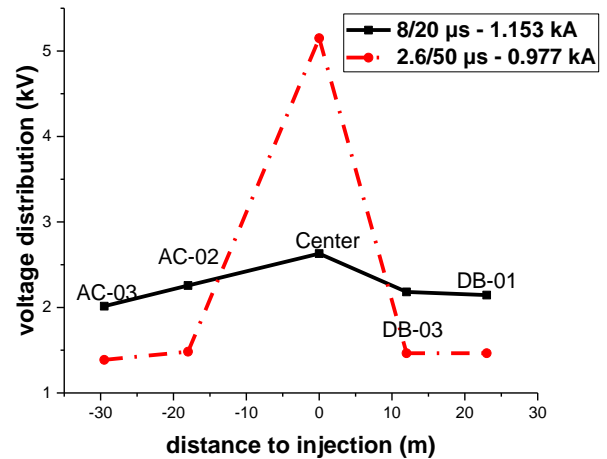


Figure 6. Voltage distribution of horizontal observations with different injecting position

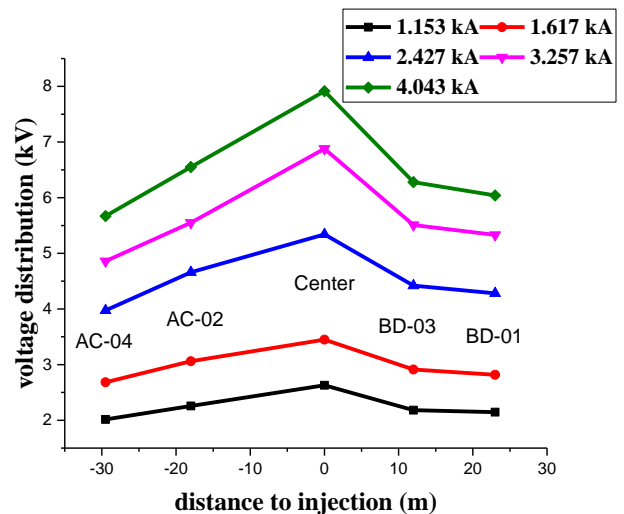


Figure 7. Voltage distribution of horizontal observations with different injecting amplitudes

IV. DISCUSSION

A. Transient and Power Frequency Characteristic Comparison

In order to compare grounding performance between transient condition and power frequency, an 8-amperes (RMS) 50 Hz current is injected from the center and border of the grounding mesh independently. Resistance and voltage distribution could be derived afterwards.

Five grounding resistances and voltage distributions are calculated and concluded. Power frequency current and a roughly 1 kA 8/20 μ s impulse current are injected into the grounding grid from the center and the border independently; a 2.6/50 μ s current close to 1 kA is injected from the center. It has been proven that under power frequency working condition, no soil ionization phenomenon would interfere with grounding performance, because it was caused by high amplitude and short rising time. Thus, voltage distribution brought by 1 kA current could be calculated proportionally by that caused by 8 A 50 Hz current. Testing conditions are summarized in TABLE III.

TABLE III. TESING CONDITIONS

Case Number	Waveform	Injecting Position	Amplitude (A)
1	50 Hz	Center	8
2	50 Hz	Border	8
3	8/20 μ s	Center	1190
4	8/20 μ s	Border	1172
5	2.6/50 μ s	Center	863

As shown in Figure 8. , 50 Hz resistance is the lowest and irrelevant to the current injecting position. As the waveform becomes steeper, resistance would rise dramatically. Also, the resistance is sensitive to injection position. When the position is at center, the whole grids has the most utilization ratio, thus having a lower impulse resistance.

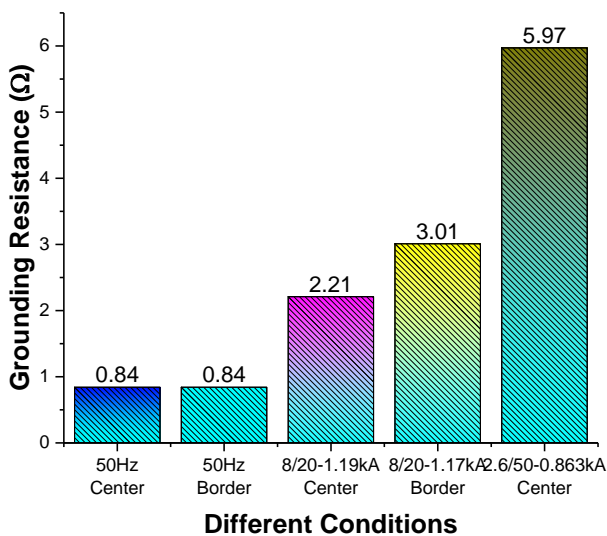


Figure 8. Grounding resistances comparison

From Figure 9. , it can be inferred that under power frequency condition, the grounding system has a relatively even potential distribution while in high frequency situation, voltage of conductors is distributed unbalanced. What's more, this unbalanced voltage would create a very high impulse step voltage near the current injecting point.

When the injecting current only has low frequency component, grounding electrodes has barely any inductive effect, all the conductor potential stays at a low level and distributed evenly as the effective area does not change. However, for impulse current with short front time consists of many high frequency components, high level potential is concentrated close to the current injection because of the inductance, causing an unbalanced potential of the whole area.

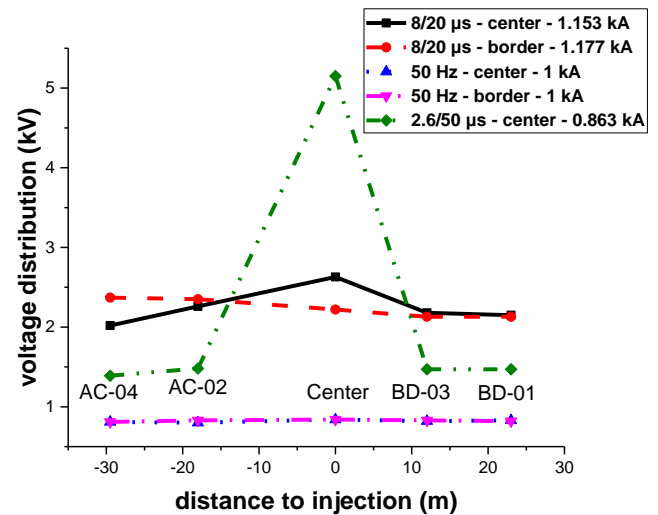


Figure 9. Voltage distribution of conductors on horizontal observations

B. Nature of Transient Characteristic

In this paper, influence of feeding position, front time and amplitude to impulse feature is studied. However, impact of these parameters is superficial. By its very nature, transient characteristic has a close relationship with inductive effect and soil ionization phenomenon. Because of inductive feature of the electrode, longitudinal current along the electrode is impeded by the reactance, which makes the current disperse into the soil nearby the injecting position. In this way, only part of the conductor is used for the current to flow so the effective area of the grounding grid is impaired. When subjecting a transient current with relative high amplitude, soil tends to be ionized, which is equivalent to enlarge the radius thus improving the performance of the earthing system. Grounding performance is depended on the trade-off of the two natural factors.

Changing impulse current feeding point would alter the utilization of grounding mesh. When current is fed into the center, all the directions could be utilized to dissipate current, thus the grounding grid having a lower transient grounding resistance. The voltage distribution is also affected by the

position of feeding point as the high level potential will be concentrated close to the current injecting point.

Front time of the waveform plays an important role in the transient characteristic because it directly relates to the current frequency. As waveform becomes steeper, frequency and inductive component rise potentially, which increasingly decreases the utilization area. So the impulse grounding resistance become higher and the voltage has a more uneven distribution.

Under transient situation, current amplitude has a close relationship with spark discharge. So as peak value of the current rises, transient resistance decreases and the voltage distribution of the whole area would increase.

V. CONCLUSION

In order to obtain a comprehensive impulse characteristic of grounding system, a large-scale impulse test platform is built in this paper, and field tests are conducted on a grounding grid of a 110kV substation. The transient characteristics of grounding grid include not only transient resistance but also voltage distribution, and their relationships with injecting points, current amplitude and waveform are considered.

Test results proves that inductive effect and soil ionization make transient characteristic of grounding grid dramatically different from the power frequency performances. High frequency lightning current and current's injecting at the border of the grid would causes significant inductive effect that might decrease the effective area. As a result, grounding resistance would rise and potential distribution on the conductors becomes uneven. Soil ionization is the consequence of short rising time and high amplitude of the feeding current helping to reduce the grounding resistance and level the potential distribution.

REFERENCES

- [1] A. C. Liew and M. Darveniza, "Dynamic model of impulse characteristics of concentrated earth," *Proc. Inst. Elect. Eng.*, vol. 121, no. 2, pp. 123–135, Feb. 1974.
- [2] R. Kosztaluk, M. Loboda, and D. Mukhedkar, "Experimental study of transient ground impedances," *IEEE Trans. Power App. Syst.*, vol. PAS-100, no. 11, pp. 4653–4660, Nov. 1981.
- [3] Gupta, B. R., and B. Thapar, "Impulse Impedance of Grounding Grids," *Power Apparatus and Systems, IEEE Transactions on*, vol. pas-99, no. 6, pp. 2357-2362, Feb. 2007
- [4] Geri, A., G. M. Veca, E. Garbagnati and G. Sartorio, "Non-linear behaviour of ground electrodes under lightning surge currents: computer modelling and comparison with experimental results," *IEEE Transactions on Magnetism*, vol. 28, no. 2, pp. 1442-1445, Mar. 1992.
- [5] A. P. Meliopoulos and M. G. Moharam, "Transient analysis of grounding system," *IEEE Trans. Power App. Syst.*, vol. PAS-102, no. 2, pp. 389–399, Feb. 1983.
- [6] Mazzetti C, Veca G M, "Impulse behaviour of grounding electrodes," *IEEE Trans. on Power. Apparatus and Systems*, vol. 102, no. 9, pp. 3148-3154, Sep. 1983.
- [7] Jinpeng Wu, Bo Zhang, Jinliang He and Rong Zeng, "A Comprehensive Approach for Transient Performance of Grounding System in the Time Domain," *IEEE Transactions on Electromagnetic Compatibility*, vol. 57, no. 2, pp. 1-7, Nov. 2014.
- [8] Bo Zhang, Jinliang He, Jae-Bok Lee, Xiang Cui, Zhibin Zhao, Jun Zou and Sug-Hun Chan, "Numerical analysis of transient performance of grounding systems considering soil ionization by coupling moment method with circuit theory," *IEEE Transactions on Magnetism*, vol. 41, no. 5, pp. 1440-1443, May 2005.
- [9] B. Nekhou, C. Guerin, P. Labie, G. Meunier, R. Feuillet and X. Brunotte, "A Finite Element Method for Calculating the Electromagnetic Field Generated by Substation Grounding Systems," *IEEE Transactions on Magnetism*, vol. 31, no. 3, pp. 2150-2153, May 1995.
- [10] Li, Jingli, Tao Yuan, Qing Yang, Wenxia Sima, Caixin Sun and Markus Zahn, "Numerical and Experimental Investigation of Grounding Electrode Impulse-Current Dispersal Regularity Considering the Transient Ionization Phenomenon," *IEEE Transactions on Power Delivery*, vol. 26, no. 4, pp. 2647-2658, Aug. 2011.
- [11] Baba, Y., N. Nagaoka, and A. Ametani, "Modeling of Thin Wires in a Lossy Medium for FDTD Simulations," *IEEE Transactions on Electromagnetic Compatibility*, vol. 47, no. 1, pp. 54-60, Feb. 2005
- [12] Masanobu Tsumura, Yoshihiro Baba, Naoto Nagaoka and Akihiro Ametani, "FDTD Simulation of a Horizontal Grounding Electrode and Modeling of its Equivalent Circuit," *IEEE Transactions on Electromagnetic Compatibility*, vol. 48, no. 4, pp. 817-825, Nov. 2006.
- [13] Taku Noda, "A Numerical Simulation of Transient Electromagnetic Fields for Obtaining the Step Response of a Transmission Tower Using the FDTD Method," *IEEE Transactions on Power Delivery*, vol. 23, no. 2, pp. 1262-1263, Apr. 2008.
- [14] G. Ala, P. L. Buccheri, P. Romano and F. Viola, et al, "Finite difference time domain simulation of earth electrodes soil ionisation under lightning surge condition," *IET Science Measurement Technology*, vol. 2, no. 3, pp. 134-145, May 2008
- [15] Greev, L., and F. Dawalibi, "An electromagnetic model for transients in grounding systems," *IEEE Transactions on Power Delivery*, vol. 5, no. 4, pp. 1773-1781, oct. 1900.
- [16] L. D. Greev and M. Heimbach, "Frequency dependent and transient characteristics of substation grounding systems," *IEEE Trans. Power Del.*, vol. 12, no. 1, pp. 172–178, Jan. 1997.
- [17] Bungler, R., and F. Arndt, "Efficient MPIE approach for the analysis of three-dimensional microstrip structures in layered media," *IEEE Transactions on Microwave Theory & Techniques*, vol. 45, no. 8, pp. 1141-1153, Aug. 1997.
- [18] Visacro, S., and A. Soares, "HEM: a model for simulation of lightning-related engineering problems," *IEEE Transactions on Power Delivery*, vol. 20, no. 2, pp. 1206-1208, Apr. 2005.
- [19] Tu, Youping, J. He, and R. Zeng, "Lightning impulse performances of grounding devices covered with low-resistivity materials," *IEEE Transactions on Power Delivery*, vol. 21, no. 3, pp. 1706-1713, July 2006.
- [20] Bellaschi, P. L., R. E. Armington, and A. E. Snowden, "Impulse and 60-Cycle Characteristics of Driven Grounds – II," *Transactions of the American Institute of Electrical Engineers*, vol. 61 no. 6, pp. 349-363, June 1942.
- [21] Harid, N., et al, "Experimental Investigation of Impulse Characteristics of Transmission Line Tower Footings," *Journal of Lightning Research*, vol. 4, no. 1, pp. 36-44, 2012.
- [22] Rong Zeng, Xuehai Gong, Jinliang He, Bo Zhang and Yanqing Gao, "Lightning Impulse Performances of Grounding Grids for Substations Considering Soil Ionization," *IEEE Transactions on Power Delivery*, vol. 23, no. 2, pp. 667-675, Apr. 2008.